Eur. Phys. J. B **59**, 109–114 (2007)
DOI: 10.1140/epjb/e2007-00257-5

THE EUROPEAN PHYSICAL JOURNAL B

Spatiotemporal chaos control in two-wave driven systems

G. Tang[1,2] and G. Hu[1,3,a]

[1] Department of Physics, Beijing Normal University, 100875 Beijing, P.R. China
[2] College of Physics and Electronic Engineering, Guangxi Normal University, 541004 Guilin, P.R. China
[3] Beijing-Hong Kong-Singapore Joint center of Nonlinear and Complex Systems Beijing Normal University Branch-Beijing, P.R. China

Received 13 December 2006 / Received in final form 4 August 2007
Published online 28 September 2007 –

Abstract. Spatiotemporal chaos control is considered by taking a one-dimensional driven/damped nonlinear drift-wave equation as a model. We apply an additional sinusoidal wave to suppress spatiotemporal chaos, and the system becomes a two-sinusoidal-wave driven system (the original driving wave with frequency ω and an additional controlling wave with frequency Ω). Numerical simulations show that when the frequency of the controlling wave is in the proper range, spatiotemporal chaos can be modified into a regular state where the amplitudes of all modes vary periodically with frequency $\Omega-\omega$ while the phases of all modes evolve quasi-periodically with a running frequency Ω overlapped by a small modulation of frequency $\Omega-\omega$. The physical reason for this peculiar phenomenon is attributed to a frequency entrainment in the competition of the two external waves.

PACS. 05.45.Gg Control of chaos, applications of chaos – 47.27.Rc Turbulence control – 52.35.Kt Drift waves

1 Introduction

Controlling spatiotemporal chaos (STC) has attracted much attention from scientists and technologists in recent years because of its potential applications in fields as diverse as hydrodynamics [1–3], plasma physics [4–6], laser systems [7], reaction-diffusion systems [8,9], and biological systems [10]. Chaos and turbulence are often considered as troublesome features in plasma devices. Therefore, elimination of such behavior in these systems is a crucial goal with many potential benefits. In this paper, we consider turbulence control by taking a plasma system as our model. Specifically, we apply an additional sinusoidal wave (controlling wave with frequency Ω) to suppress STC in a one-dimensional nonlinear drift-wave equation driven by a sinusoidal wave (driving wave with frequency ω), which drives the system towards a spatiotemporal chaotic state. We investigate the mechanism through which the controlling wave acts. It is observed that the controlling wave has a suppressive effect on the chaotic dynamics of the unperturbed system if the frequency of the controlling wave is in the correct range. More significantly, we observe the occurence of frequency entrainment. Under successful STC suppression, the system is driven to such a quasi-periodic state that the phases of all the modes rotate at the high frequency Ω with small perturbed oscillations at the difference frequency $\Omega-\omega$. Meanwhile, the amplitudes of the modes and the energy of the system oscillate periodically at this difference frequency. This interesting behavior can be intuitively understood using the concepts of frequency entrainment and phase locking to a moving frame fixed to the controlling wave.

This paper is organized as follows. In Section 2 we describe the dynamical model and the STC control results from numerical simulations. In Section 3 we describe the physical mechanism underlying this STC control method and the related frequency entrainment phenomenon. A discussion is presented in the last section.

2 Model and numerical results of STC control

In this section, we consider the problem of controlling drift-wave STC in a one-dimensional nonlinear drift-wave equation through an additional sinusoidal wave. The dynamic equation reads

$$\frac{\partial\phi}{\partial t}-a\frac{\partial^3\phi}{\partial t\partial x^2}+c\frac{\partial\phi}{\partial x}+f\phi\frac{\partial\phi}{\partial x}= -\gamma\phi-\varepsilon\sin(x-\omega t)-g\sin(x-\Omega t), \quad (1)$$

where ϕ is a fluctuating electric potential. The 2π boundary condition is applied and $a=0.2871$, $\gamma=0.1$, $c=1.0$,

[a] e-mail: ganghu@bnu.edu.cn

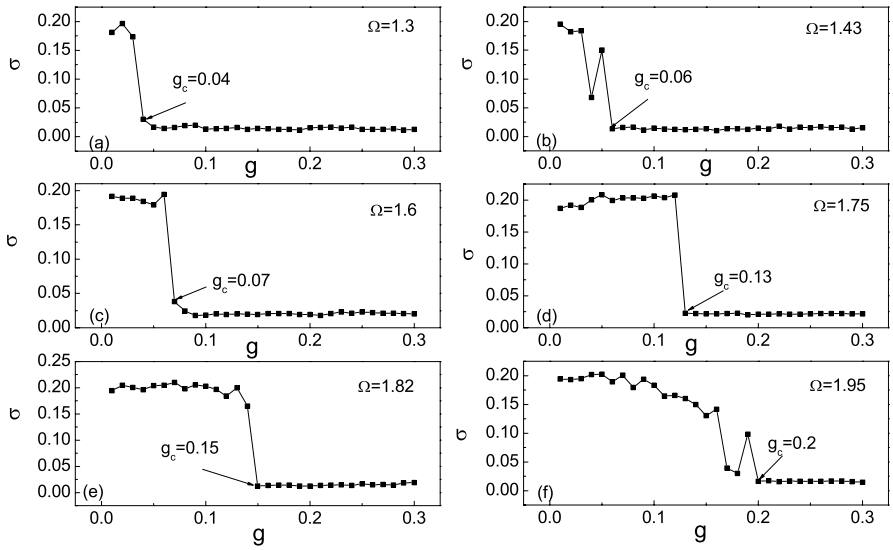

Fig. 1. Control error σ as defined by equation (3) vs. control strength g for different values of Ω (a) $\Omega = 1.3$. (b) $\Omega = 1.43$. (c) $\Omega = 1.6$. (d) $\Omega = 1.75$. (e) $\Omega = 1.82$. (f) $\Omega = 1.95$.

$f = -6.0$, $\varepsilon = 0.22$ and $\omega = 0.65$ are fixed throughout the paper. The two adjustable control parameters are Ω and g, where g is referred to as the control strength. We refer to $\sin(x - \omega t)$ as the driving wave and $\sin(x - \Omega t)$ as the controlling wave. Without the control term ($g = 0$) equation (1) describes the drift-wave dynamics in magnetized bounded plasmas [11], and STC is observed for the above set of parameters [11,12]. In recent years, various feedback control methods - including local feedback injections [13,14] and time-delay feedback control [15] – have been proposed to suppress STC in this system. All these feedback methods require instantaneous measurements of the system properties as well as instantaneous signal injections depending on the measurements. In practice, it may be difficult to meet these requirements. The new research in this paper consists of the examination of a non-feedback method, i.e., the investigation of how an additional wave can tame STC. This work is a significant extension of the well-known non-feedback control of low-dimensional chaos [16,17] to non-feedback STC control in high-dimensional spatiotemporal systems by two periodic control waves. In the numerical simulations, we apply a method of dividing the space of 2π into $N = 256$ grids. The time increment Δt is chosen to be 10^{-3}. The total integration time length of each simulation run is 2500. The result of the numerical algorithm is verified by using smaller space and time steps (almost identical results are obtained for the two different precisions: $N = 256$, $\Delta t = 10^{-3}$ and $N = 512$, $\Delta t = 0.5 \times 10^{-3}$). The initial distribution of ϕ does not affect the asymptotic state of the system. In the present work we take an arbitrary initial distribution of ϕ with $\bar{\phi} = \frac{1}{2\pi}\int_0^{2\pi} \phi(x,t)dx = 0$. Any nonzero integral damps to zero with time, and zero integral remains after the entire dynamic evolution. The control is not added until equation (1) with $g = 0$ has been integrated to $t = 500$, ensuring that the system has past the transient stage and reached a STC state.

In plasma physics, the wave energy of the system

$$E(t) = \frac{1}{2\pi}\int_0^{2\pi} \frac{1}{2}\left[\phi^2(x,t) + a\left(\frac{\partial\phi(x,t)}{\partial x}\right)^2\right] dx \quad (2)$$

is conveniently used to monitor the dynamics of the system. Without the controlling wave ($g = 0$), the system shows STC and $E(t)$ varies chaotically over a large range. In order to characterize the control effect, we define the quantity of control error as

$$D(t_n) = \underbrace{\min}_{n_0 \in (104, n-1)} \left[\frac{1}{N}\sum_{i=1}^{N} |\phi(x_i, n_0 T_\omega) - \phi(x_i, nT_\omega)|\right],$$

$$T_\omega = \frac{2\pi}{\omega}, \quad \sigma = \frac{1}{10}\sum_{n=249}^{258} D(t_n), \quad (3)$$

where $D(t_n)$ takes the minimum value of the differences of $\sum_{i=1}^{N} |\phi(x_i, n_0 T_\omega) - \phi(x_i, nT_\omega)|$, $n_0 = 104, 105, \cdots, n-1$, respectively. The particular numbers 104, 249 and 258 have no special physical meanings. They are arbitrarily chosen to satisfy the condition that any transient of the control process has been discarded. The control error σ measures the deviation from periodicity. When STC is successfully suppressed, σ decreases from a large value to a small one, and the system reaches a quasi-periodic state with periods of $(\frac{2\pi}{\omega}, \frac{2\pi}{\Omega})$.

Now we focus on the control performance of the controlling wave. First, we numerically compute the control error σ for different values of Ω and g. In Figure 1 we plot σ vs. control strength g for varying Ω. It is observed

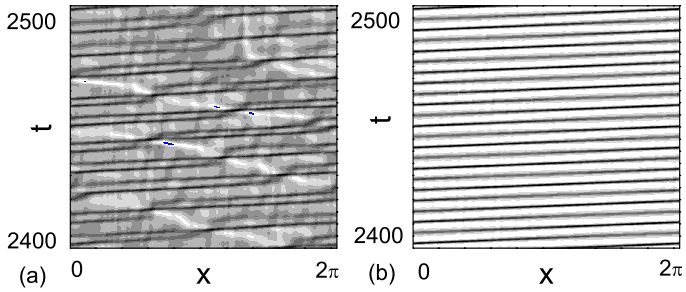

Fig. 2. Spatiotemporal patterns of $\phi(x,t)$ from equation (1) when $\Omega = 1.43$ is applied. (a) $g = 0.01$, STC pattern is observed. (b) $g = 0.06$, STC is suppressed, and quasi-periodic pattern is realized.

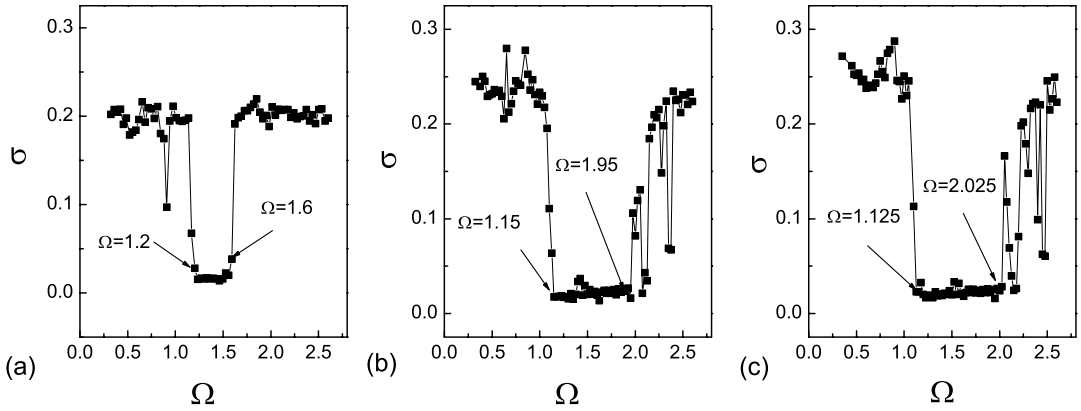

Fig. 3. Control error σ vs. Ω for different control strengths, g. (a) $g = 0.07$. (b) $g = 0.20$. (c) $g = 0.24$.

that STC can be successfully suppressed by a controlling wave given a proper choice of g and Ω. There exists a critical control strength g_c for successful control and g_c increases as Ω increases. When STC has been suppressed, σ decreases to small but nonzero values and the system reaches a quasi-periodic state. To demonstrate the control effect, we present two spatiotemporal patterns of $\phi(x,t)$ in Figure 2 where Figures 2a and 2b correspond to parameter sets from Figure 1 with large and small σ, respectively. It is obvious that the former state is STC while the latter one is a regular and non-chaotic state, where the original STC (for $g = 0$) is suppressed by the controlling wave. In Figure 3 we plot control error σ vs. frequency Ω for different $g's$. One can observe that for a given control strength there exists a window of frequencies Ω for the successful suppression of STC. It is well known that in low-dimensional systems subjected to two harmonic forces, a resonance condition (ratio of the frequencies of the two harmonic forces must be an integer or rational number) [16,17] is crucial for chaos suppression. However, in our work we find interestingly that the parameter regions for STC suppression in Figure 3 are actually independent of the resonance condition. This is in strong contrast with the conventional view of chaos suppression. We find that this is a characteristic feature of STC suppression in double-wave driven spatiotemporal systems, which cannot exist in low-dimensional systems. This conclusion will be explained heuristically in next section.

In order to demonstrate the control effect in a more systematic manner, we plot $E_{\max}$ against g for different values of Ω in Figure 4, where $E_{\max}$ is the maximum energy value in the asymptotic evolution of $E(t)$ for the given parameter set. In Figure 5 we plot $E_{\max}$ vs. frequency Ω for different values of g. Figures 4 and 5 show the interesting phenomenon that energy $E(t)$ varies periodically (i.e., $E_{\max}$ takes a single value for a fixed parameter set) when the STC is successfully suppressed, though the system is driven quasi-periodically by two waves with two irreducible frequencies. It should be noted that we have an irrational value for Ω/ω (with probability equal to one) in the periodic regions of Figure 5, and this periodicity can never happen for quasi-periodically driven low-dimensional systems.

To gain an intuitive impression of how changing Ω can change the control results, we plot in Figure 6 the asymptotic states of ϕ for different values of Ω which are a rational multiple of the driving frequency ω. It is observed that in all the cases shown in Figures 6a, 6b and 6c, STC can be suppressed and periodic motions with period $T = k\frac{2\pi}{\omega} = K\frac{2\pi}{\Omega}$ are realized with little imperfection. Here k and K are integers with $\frac{K}{k} = \frac{\Omega}{\omega}$.

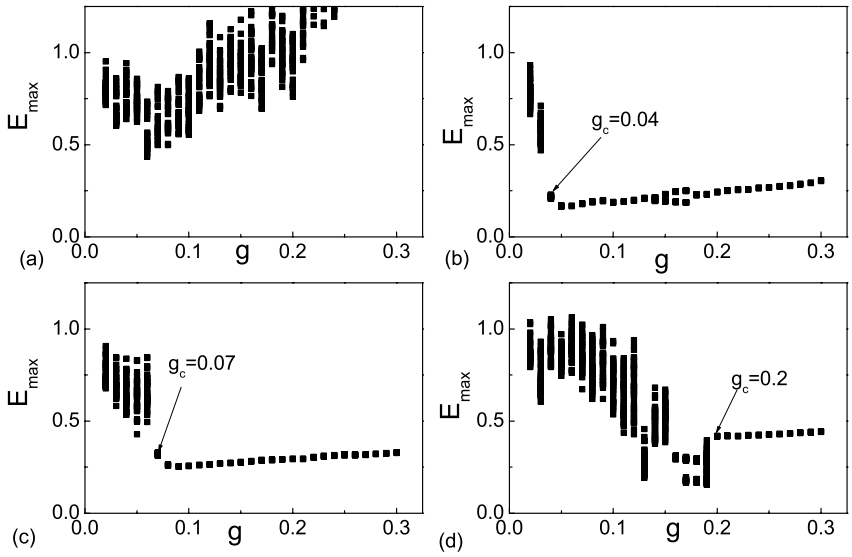

Fig. 4. $E_{\max}$ vs. g for different values of Ω where $E_{\max}$ is defined as the maximum value in the asymptotic evolution of $E(t)$. In each run, $E_{\max}$ is recorded after $t \geq 2200$. (a) $\Omega = 0.52$. (b) $\Omega = 1.3$. (c) $\Omega = 1.6$. (d) $\Omega = 1.95$. In case (a), STC cannot be suppressed through use of a controlling wave.

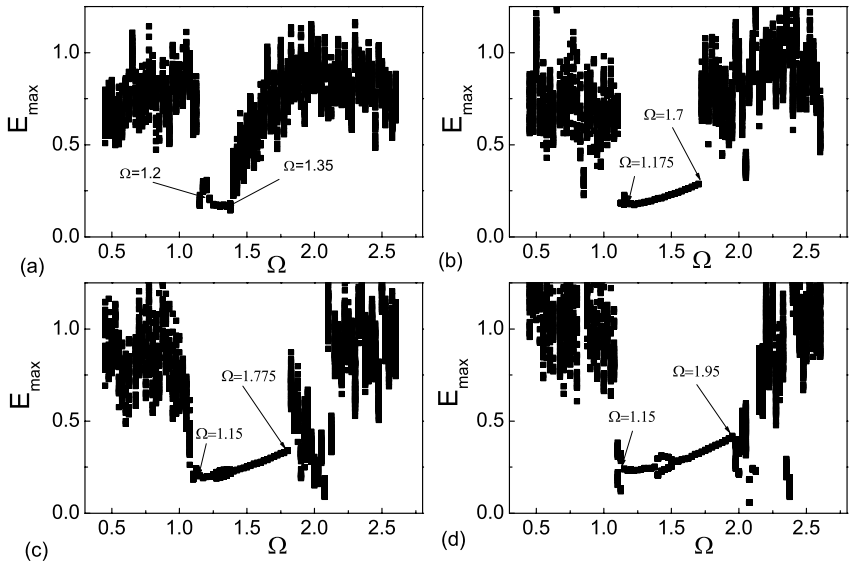

Fig. 5. The same as Figure 4 with $E_{\max}$ vs. Ω for different values of g. (a) $g = 0.05$. (b) $g = 0.10$. (c) $g = 0.15$. (d) $g = 0.20$. The periodicity of $E(t)$ results in the smooth curves in the "controllable" windows, in sharp contrast with the random and scattered plots in the STC domains.

3 Frequency entrainment and phase locking

To analyze the mechanism of STC suppression, we study the solution of equation (1) in Fourier space. By inserting the Fourier transformation of ϕ

$$\phi(x,t) = A_0 + \sum_{m=1}^{\infty} A_m(t)\cos(mx - \beta_m(t)), \qquad (4)$$

into equation (1) and setting $\bar{\phi} = 0$ we have

$$(1+am^2)\frac{\partial A_m}{\partial t} = W_m(t) - \gamma A_m - \varepsilon\delta_{m,1}\sin(\beta_1 - \omega t) - g\delta_{m,1}\sin(\beta_1 - \Omega t), \qquad (5a)$$

$$(1+am^2)A_m\frac{\partial \beta_m}{\partial t} = Q_m(t) - cmA_m - \varepsilon\delta_{m,1}\cos(\beta_1 - \omega t) - g\delta_{m,1}\cos(\beta_1 - \Omega t), \qquad (5b)$$

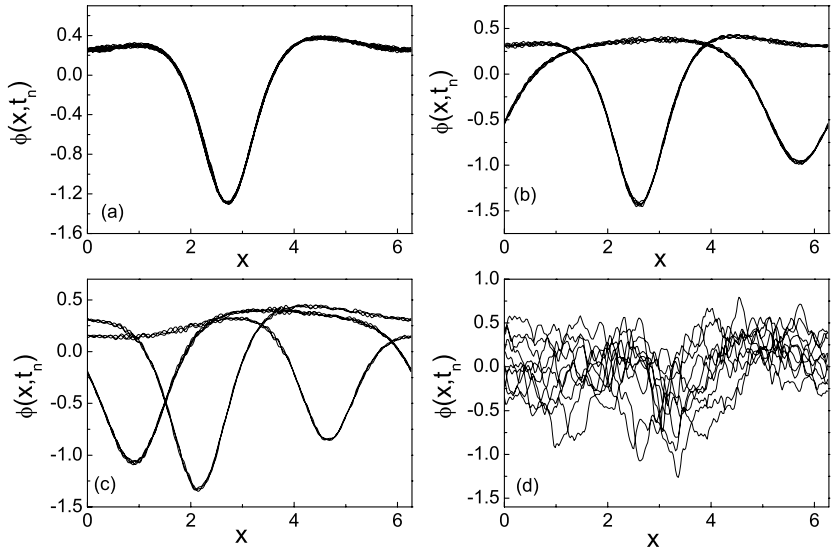

Fig. 6. Snapshots of $\phi(x,t)$ at various times $t = t_n = nT_\omega$, $T_\omega = \frac{2\pi}{\omega}$ and $n \in [249, 258]$. (a) $\Omega = 2\omega$, $g = 0.22$. (b) $\Omega = \frac{5}{2}\omega$, $g = 0.22$. (c) $\Omega = \frac{7}{3}\omega$, $g = 0.22$. (d) $g = 0.0$ (without control). When STC is successfully suppressed, all system states become almost periodic with period $T = k\frac{2\pi}{\omega} = K\frac{2\pi}{\Omega}$. Here k and K are integers.

where

$$W_m(t) = \frac{fm}{4}\left\{\sum_{i+j=m} A_i A_j \sin(\beta_m - \beta_i - \beta_j) + \sum_{j-i=m} A_i A_j \sin(\beta_m - \beta_j + \beta_i) + \sum_{i-j=m} A_i A_j \sin(\beta_m - \beta_i + \beta_j)\right\}, \quad (6a)$$

$$Q_m(t) = \frac{fm}{4}\left\{\sum_{i+j=m} A_i A_j \cos(\beta_m - \beta_i - \beta_j) + \sum_{j-i=m} A_i A_j \cos(\beta_m - \beta_j + \beta_i) + \sum_{i-j=m} A_i A_j \cos(\beta_m - \beta_i + \beta_j)\right\}, \quad (6b)$$

(m,i,j=1,2,3...) under

$$\delta_{m,1} = \begin{cases} 1 \text{ if } m = 1, \\ 0 \text{ other.} \end{cases}$$

From equation (5), one may observe that the driving and controlling waves only directly drive the mode with wave number $m = 1$, and all other modes are driven by the external waves indirectly through mode-mode interactions from modes of low wave numbers. In order to understand the effects of the two forces, we present in Figure 7 the time evolution of $E(t)$, $\phi(x,t)$, $A_m(t)$, and $\beta_m(t)$ $(m \leq 4)$ when STC has been well-suppressed asymptotically. The most interesting feature is the frequency entrainment of the system by the controlling wave. All the β_m rotate with frequencies entrained to frequencies $m\Omega$, $m = 1, 2, \cdots$, respectively (i.e., the motion of the phases of all modes are locked to a moving frame fixed to one of the driving waves with higher frequency), and the phase differences $\beta_m - m\Omega t$ are well locked within a range less than 2π and oscillate periodically at a frequency equal to the difference of the controlling wave frequency and the driving wave frequency $\Omega - \omega$. The amplitudes of modes and the energy of the system, however, oscillate periodically at this difference frequency $\Omega - \omega$. This observation confirms the interesting phenomenon shown in Figures 4 and 5, that the energy $E(t)$ varies periodically while the two external waves provide quasi-periodic driving. Another interesting observation is that all amplitudes $A_m(t)$ and the phase differences $\beta_m - m\Omega t$ have almost identical phase behavior during the oscillations. From our investigation, it is found that in all the cases of Figures 1, 3, 4, and 5, frequency entrainment and phase locking are directly associated with the controllability transition of the system from STC to quasi-periodicity.

4 Discussion

In this concluding section, let us explain how a spatiotemporal system driven by quasi-periodical waves can have perfect periodicity in many important quantities, such as energy $E(t)$, and mode amplitudes A_m in our case. Fundamentally, any quantity of a system driven quasi-periodically should evolve quasi-periodically. In order for some quantities of such a system to show periodicity, there must exist some mechanism separating the two (or more) driving frequencies. This mechanism clearly exists in the two-wave driven extended system equation (1). The key

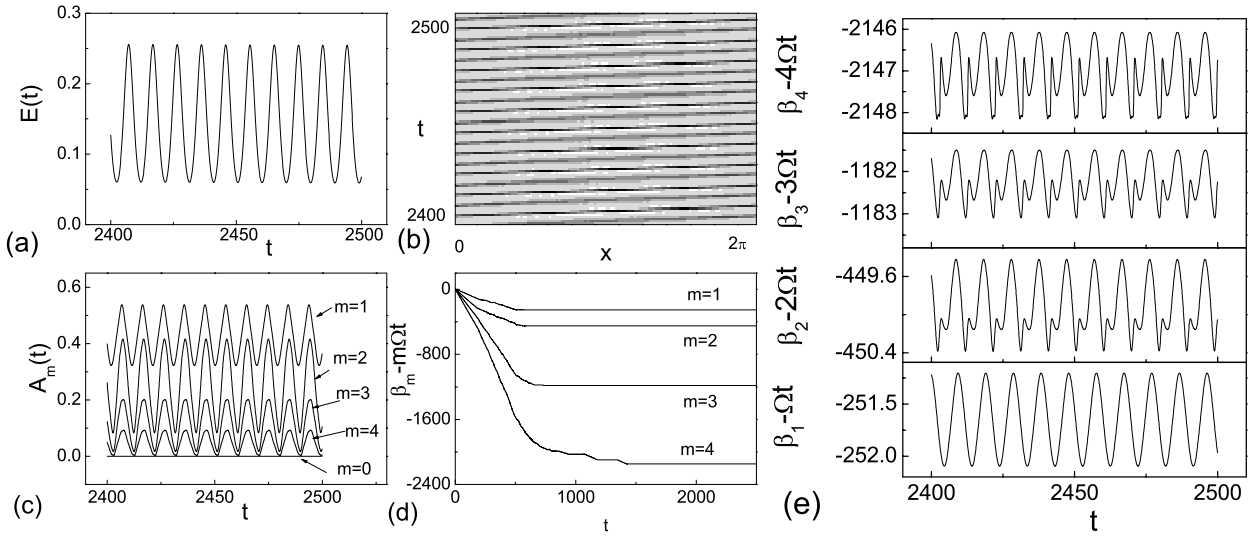

Fig. 7. Characteristic features of STC suppression for $g = 0.22$ and $\Omega = 1.3$. (a) Time evolution of $E(t)$. (b) Spatiotemporal evolution of potential $\phi(x,t)$. (c) Evolution of amplitudes A_m as defined in equation (4). (d-e) Evolution of phase differences $\beta_m - m\Omega t$.

point is frequency entrainment, which can be most conveniently explained by a transformation from the static frame (x,t) to the moving frame (y,t) with

$$y = x - \Omega t. \tag{7}$$

Inserting (7) into (1) we have

$$\frac{\partial\phi(y,t)}{\partial t} - a\frac{\partial^3\phi}{\partial t\partial y^2} + c\frac{\partial\phi}{\partial y} + f\phi\frac{\partial\phi}{\partial y} - \Omega\frac{\partial}{\partial y}\left(1 - a\frac{\partial^2}{\partial y^2}\right)\phi = -\gamma\phi - \varepsilon\sin[y + (\Omega - \omega)t] - g\sin(y),$$

this equation is periodically driven (the controlling forcing function becomes stationary in the moving frame). When STC is successfully controlled, most probably, the motion of $\phi(y,t)$ is periodic, following the periodic forcing function of frequency $\Omega - \omega$, $\varepsilon\sin[y + (\Omega - \omega)t]$. It is thus not strange that the quantities of $E(t)$ and $A_m(t)$ vary periodically with frequency $\Omega - \omega$.

Moreover if we expand $\phi(y,t)$ via Fourier transformation, and $\phi(y,t) = \sum_{m=0}^{\infty} A_m(t)\cos(my + \alpha_m(t)) = \sum_{m=0}^{\infty} A_m(t)\cos(mx - m\Omega t + \alpha_m(t))$ we find that the two frequencies of Ω and ω perform well-separated functions, i.e., one frequency $\Omega - \omega$ determines the periodic variation of amplitudes $A_m(t)$ and the periodic oscillation of phases $\alpha_m(t)$, and the other frequency Ω determines the phase rotations of $\beta_m(t)$ only.

In summary, chaos suppression in equation (8) causes a transition from STC to a periodic wave in a moving frame. Transforming back to the static frame with equation (7), the state of equation (1) becomes the quasi-periodic state with frequency entrainment of Figures 6 and 7 where the system energy and field amplitudes show periodicity, as well as quasi-periodic phase evolution.

This work was supported by National 973 project of Nonlinear Science and the Natural Science Foundation of China (Grant Nos. 10335010).

References

1. O. Lüthje, S. Wolff, G. Pfister, Phys. Rev. Lett. **86**, 1745 (2001)
2. S. Guan, G.W. Wei, C.H. Lai, Phys. Rev. E **69**, 66214 (2004)
3. G. Tang, G. Hu, Phys. Rev. E **73**, 56307 (2006)
4. E. Gravier, X. Caron, G. Bonhomme, T. Pierre, Phys. Plasma **6**, 1670 (1999)
5. T. Klinger, C. Schröder, D. Block, F. Greiner, A. Piel, G. Bonhomme, V. Naulin, Phys. Plasma **8**, 1961 (2001)
6. C.F. Figarella, A.K. Sen, S. Benkadda, P Beyer, X. Garbet, Plasma Phys. Control. Fusion **45**, 1297 (2003)
7. L. Pastur, L. Gostiaux, U. Bortolozzo, S. Boccaletti, P.L. Ramazza, Phys. Rev. Lett. **93**, 63902 (2004)
8. V. Petrov, M.J. Crowley, K. Showalter, Phys. Rev. Lett. **72**, 2955 (1994)
9. C.K. Tung, C.K. Chan, Phys. Rev. Lett. **89**, 248302 (2002)
10. K. Hall, D.J. Christini, M. Tremblay, J.J. Collins, L. Glass, J. Billette, Phys. Rev. Lett. **78**, 4518 (1997)
11. He Kaifen, A. Salat, Plasma Phys. Control. Fusion **31**, 123 (1989)
12. Kaifen He, Phys. Rev. E **59**, 5278 (1999)
13. H. Guang, H. Kaifen, Phys. Rev. Lett. **71**, 3794 (1993)
14. Hu Kaifen, Hu. Gang, Phys. Rev. E **53**, 2271 (1996)
15. G. Tang, K. He, G. Hu, Phys. Rev. E **73**, 56303 (2006)
16. Z. Qu, G. Hu, G. Yang, G. Qin, Phys. Rev. Lett. **74**, 1736 (1995)
17. R. Chacón, Phys. Rev. Lett. **86**, 1737 (2001)